THE JOURNAL OF PHYSICAL CHEMISTRY B LETTERS

2006, *110,* 16185−16188
Published on Web 08/03/2006

Highly Dispersed Pt Catalysts on Single-Walled Carbon Nanotubes and Their Role in Methanol Oxidation

Anusorn Kongkanand,[†,‡] K. Vinodgopal,[*,†,§] Susumu Kuwabata,[*,‡] and Prashant V. Kamat[†]

Radiation Laboratory, Departments of Chemistry & Biochemistry and Chemical & Biomolecular Engineering, University of Notre Dame, Notre Dame, Indiana 46556-0579, Department of Applied Chemistry, Graduate School of Engineering, Osaka University, Suita, Osaka 565-0871, Japan, and Department of Chemistry, Indiana University Northwest, Gary, Indiana 46408

Received: June 28, 2006; In Final Form: July 20, 2006

Well-dispersed Pt catalysts with very high utilization efficiencies for fuel cell reactions have been prepared by ethylene glycol reduction on polymer-wrapped single-walled carbon nanotubes (SWCNTs). By wrapping the SWCNTs in a polymer such as polystyrene sulfonate, we are able to break up the nanotube bundles to achieve better dispersion. These polymer-wrapped SWCNTs with platinum nanoparticles deposited on them show very high electrochemically active surface areas. The increase in utilization efficiencies for platinum catalysts on these SWCNT supports can be attributed to the increased surface areas and the well-dispersed nature of the carbon support and catalyst. The catalyst dispersion facilitates diffusion of reactant species which in turn results in higher methanol oxidation currents and more positive potentials for oxygen reduction.

Introduction

Single-walled carbon nanotubes (SWCNTs) are considered to be important building blocks in nanotechnology because of their exceptional mechanical and electronic properties. They can show either metallic or semiconductive properties depending on their graphene structure and hence are considered to be promising materials for molecular wires[1,2] and transistors.[3,4] SWCNTs can also be used for storing and transporting gas molecules. Confined water[5,6] and gas[7−9] molecules in SWCNTs are found to have exceptionally high diffusion coefficients, which can operate ballistic motion through the tube.

Recent efforts in our laboratory[10−12] and elsewhere[13−18] have focused on the utilization of carbon nanostructures as supporting materials to disperse metal electrocatalysts. Hydrogen and direct methanol fuel cells using SWCNT-based PEM assemblies show improved fuel cell performances when compared to commercial carbon black supported Pt catalysts. Our rotating disk electrode experiments on the Pt/SWCNT system points to a lower onset potential and a higher electron transfer rate constant for oxygen reduction.[19] The experiments demonstrated that the beneficial effect of SWCNTs is more than an increased surface area of the supporting materials. Its potential use as an electrocatalyst hence deserves further investigation.

When suspended in solution, pristine SWCNTs form large bundles due to the strong van der Waals interaction between nanotubes. Such a bundling effect leads to poor dispersion of metal particles on SWCNTs and limits the overall electrocatalytic activity. Thus, it is important to deposit metal nanoparticles on well-separated individual SWCNTs. However, the significant curvature of SWCNTs (mean diameter of 1.4 nm) poses a challenge to achieve this goal.

SCHEME 1: Pt Particles Dispersed on SWCNT

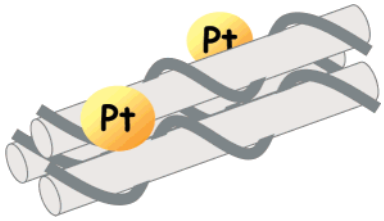

Common strategies to disperse SWCNTs are to functionalize the side wall of nanotubes[20] or to use surfactants.[21,22] O'Connell et al.[23] showed that SWCNTs can be solubilized in water with the help of linear polymers as surfactants to wrap around the SWCNTs. Functionalization of the side wall is expected to damage the intrinsic property of SWCNTs, while use of surfactant raises the possibility of contamination of the electrocatalysts.

We now report a successful method of preparing well-dispersed Pt/SWCNT electrocatalysts (Scheme 1). The Pt/SWCNT has an exceptionally high electrochemically active surface area (ECSA), exhibits excellent electrocatalytic activities toward oxygen reduction and methanol oxidation, and has potential application in designing a membrane assembly for direct methanol fuel cells (DMFCs).

Experimental Section

Solubilization of SWCNTs. SWCNTs purchased from SES Research were first refluxed in 5 M HNO_3 solution for 1 h to remove any impurity and to oxidize the opened end of the tubes,

* To whom correspondence should be addressed. E-mail: kvinod@iun.edu (K.V.); kuwabata@chem.eng.osaka-u.ac.jp (S.K.).
† University of Notre Dame.
‡ Osaka University.
§ Indiana University Northwest.

10.1021/jp064054s CCC: $33.50

thereby making them more wettable. Then, two different techniques were employed to solubilize the SWCNTs. In one method, the SWCNTs were refluxed for an additional 10 h in concentrated HNO_3/H_2SO_4 solution so as to oxidize the side wall.[20] We abbreviate the carbon nanotubes resulting from such a process as Ox-SWCNT. In the other technique, a modified polymer-wrapping procedure reported by Smalley and co-workers was employed.[23,24] In this procedure, 10 mg of pretreated SWCNTs was sonicated in 100 mL of *N*,*N*-dimethylformamide (DMF) for 15 h. Smalley et al. claim that the CNT bundles break into individual SWCNTs following sonication in DMF. Then, 20 mg of poly(sodium 4-styrenesulfonate) (PSS) was added to the suspension prior to 12 h sonication. PSS is expected to wrap around the individual SWCNTs due to a thermodynamic driving force to reduce the hydrophobic interface between the tubes and polar solvent. The SWCNTs were collected by filtration and then rinsed with water. X-ray photoelectron spectroscopic analysis of sulfur content in polymer-wrapped SWCNTs (PW-SWCNTs) estimated the presence of PSS in PW-SWCNTs to be ~40 wt %.

Preparation of SWCNT Supported Electrocatalysts. Pt colloidal solution was synthesized using the reduction of $PtCl_4^{2-}$ by ethylene glycol at pH 12.5.[25,26] The solution of Pt colloids in ethylene glycol was mixed with SWCNTs in water, and the pH of the mixture was adjusted to 4.0 to obtain 30 wt % Pt nanoparticles deposited on SWCNTs (Pt/SWCNT). The Pt/SWCNTs were filtered and dried and could be easily dispersed in water. Pt (30 wt %) on carbon black was purchased from Tanaka Kikinzoku Kougyo. For electrochemical measurements, the electrocatalysts were casted as thin films on GC electrodes with Nafion as a binder.[19]

Transmission electron microscope (TEM) images of the Pt/SWCNT samples were obtained on a Hitachi H-800SS transmission electron microscope at an accelerating voltage of 300 kV. To obtain the TEM images, a single drop of the CNT suspension was deposited on holey carbon microgrids. For X-ray photoelectron spectroscopic measurements, Pt/PW-SWCNTs were cast on a grassy carbon plate without using Nafion as a binder. The binding energy was calibrated against C1s (284 eV).

Raman spectra were obtained on two different JASCO spectrometers: a Ventuno system using a 532 nm laser excitation and a NRS 3200 system using a 785 nm laser excitation. In all cases, the spectrometer configuration used a backscattering geometry with a 100× objective lens and the CNT samples were drop cast on a silicon wafer. Spectra were obtained at a slit width of 10μ and an exposure time of 30 s.

Results and Discussion

Figure 1 shows cyclic voltammograms for H adsorption on Pt/SWCNTs prepared by the two techniques, compared with commercial Pt deposited on carbon black. Characteristic peaks in the negative region (0−0.3 V) are attributed to atomic hydrogen adsorption on the Pt surface and reflect the ECSA of Pt. Pt deposited on Ox-SWCNTs showed very little of the characteristic peaks, which disappeared after storing the Ox-SWCNT suspension for 2 weeks. Ox-SWCNTs showed a poor capability of anchoring Pt particles as expected from the high curvature of SWCNTs. In contrast, remarkably large peaks were observed on Pt/PW-SWCNTs, reflecting their high surface area. The ECSA of 118 m^2/g_{Pt} obtained with the Pt/PW-SWCNTs is about 3 times higher than that for Pt/CB and to the best of our knowledge is at least 2 times higher than any other Pt-supporting materials,[27−30] showing the effectiveness of PW-SWCNTs in dispersing Pt particles. No degradation in the ECSA was observed for the Pt/SWCNT after storing it in a suspension for over 7 months.

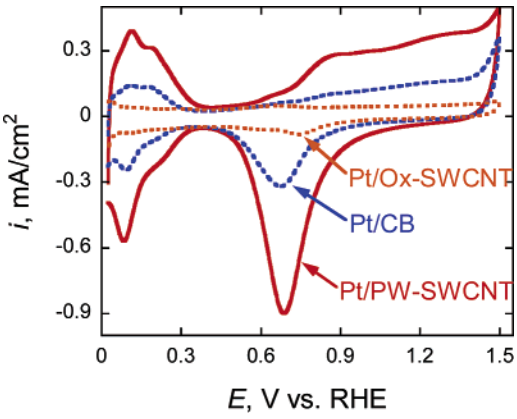

Figure 1. Cyclic voltammograms for Pt/PW-SWCNT, Pt/Ox-SWCNT, and Pt/CB recorded in 0.1 M $HClO_4$ at a scan rate of 0.02 V/s. The Pt loadings were 14 $\mu g/cm^2$.

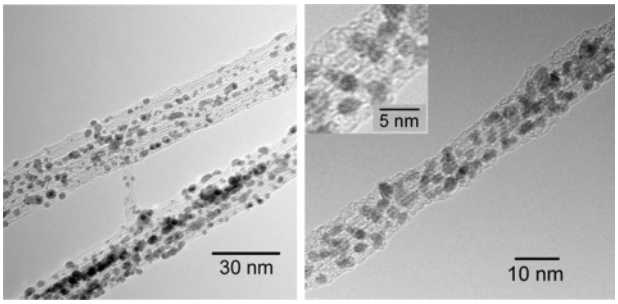

Figure 2. TEM images of Pt/PW-SWCNT at two different magnifications.

We have also obtained high resolution TEM images of the Pt/PW-SWCNT to verify the dispersion of Pt particles on the PW-SWCNT, as shown in Figure 2. An additional figure to illustrate the dispersion is shown in Supporting Information Figure S1. The PW-SWCNTs are believed to form loose bundles in water due to the electric double-layer effect of the ionic polymers. This allows the deposition of Pt particles to take place on PW-SWCNTs. The images show that 2−3 nm sized platinum particles are uniformly dispersed on the nanotube bundles. Although SWCNTs usually agglomerate when the suspension dries on the TEM grid, small bundles of 5−15 nm are easily found.

We have also used resonance Raman spectroscopy to determine the dispersion of the nanotubes. Raman spectroscopy is a powerful tool to characterize nanotubes. The ring breathing Raman active vibrational mode of nanotubes has been used to determine the diameter of the nanotubes that are in resonance with the incident laser radiation.[31−33] Figure 3 shows the resonance Raman spectrum of the PW-SWCNT samples with Pt dispersed on them using 532 and 785 nm excitation, respectively. The spectra in both cases are well resolved with a typical HWHM of ~4 cm^{-1}. The spectrum obtained with 785 nm laser excitation shows a dominant peak at 268 cm^{-1}. This is consistent with the value for nanotubes dispersed in sodium dodecyl sulfate (SDS) reported by Heller et al.[33] They attribute the 268 cm^{-1} peak to carbon nanotubes associated in tight bundles. The frequency of the ring breathing mode (RBM) is inversely proportional to the nanotube diameter. For an isolated nanotube, $\omega_r = 224/d_t$, where ω_r is the frequency of the RBM in wavenumbers and d_t is the diameter of the nanotube. However, in the case of nanotube bundles, this frequency is often shifted due to tube−tube interactions. For bundles, the

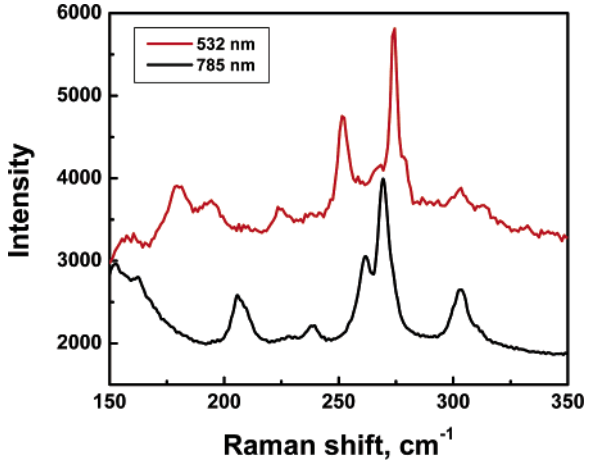

Figure 3. Raman spectra in the ring breathing mode region for the Pt/PW-SWCNT on a silicon wafer recorded with two different exciting laser wavelengths: 532 and 785 nm.

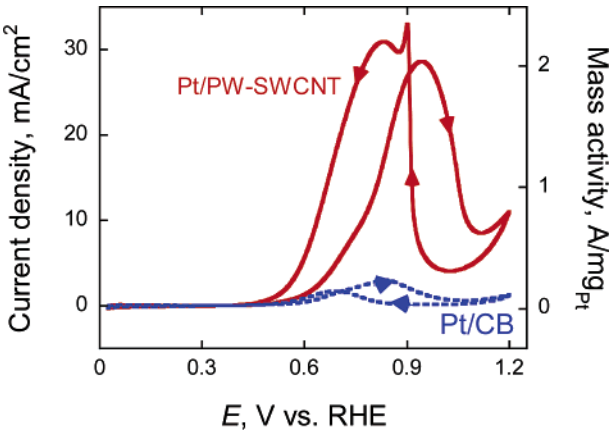

Figure 4. Cyclic voltammograms of methanol oxidation on Pt/PW-SWCNT and Pt/CB recorded in 1 M MeOH + 0.1 M $HClO_4$ at a scan rate of 0.02 V/s. The Pt loadings were 14 $\mu g/cm^2$.

relationship is $\omega_r = 223.5/d_t + 12.5\ cm^{-1}$. Using this relationship, we can estimate the diameter of the nanotubes in resonance with the incident laser wavelength. In both the 532 and 785 nm cases, we obtain nanotube diameters in the range 0.8−1.5 nm. Since the Raman signal arises only from those tubes with a band edge in resonance with the exciting laser line, the absence of larger diameter tubes cannot be precluded. However, the Raman spectrum and the TEM images indicate well-dispersed nanotubes.

One way to evaluate the accessibility of Pt to the reactants is to determine the utilization efficiency of Pt, which is the ratio of ECSA and the estimated surface area of the Pt particles. From TEM images, the mean particle size is estimated to be 2.2 nm, which gives a theoretical surface area of 127 m^2/g_{Pt} if we assume the Pt particle to be a sphere. The ECSA measured on Pt/PW-SWCNT using hydrogen adsorption voltammograms was 118 m^2/g_{Pt}, resulting in a utilization efficiency of 93%. This is exceptionally higher than those of Pt/CB (34%) and Pt/MWCNT (58%)[17] and is attributable to the unique structure of PW-SWCNTs which allow most of the Pt particles to be accessible.

Oxidation of methanol was measured using cyclic voltammetry, as shown in Figure 4. The Pt/PW-SWCNT showed a 10-fold higher peak current than the Pt/CB. This increase is significant and much higher than the increase predicted by the 3-fold difference in ECSA between the two electrodes. This indicates an increased transportation rate of the reactant, which could be related to the ballistic diffusion observed for confined

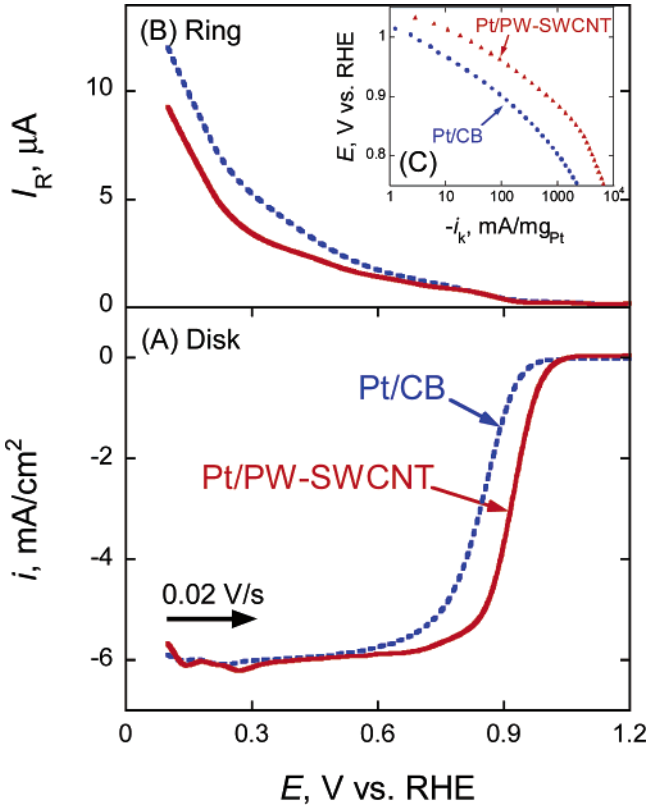

Figure 5. Disk (A) and ring (B) currents for oxygen reduction at 24 °C in O_2-saturated 0.1 M $HClO_4$ and the corresponding Tafel plot (C). Rotating rate = 1600 rpm, E_R = 1.2 V.

gas or water inside SWCNTs.[5−9] The phenomenon has not been observed on MWCNTs or oxidized SWCNTs so far.[18,34]

A good dispersion of Pt on SWCNTs gives us better insight into the latter's electrocatalytic activity and electronic property. Catalytic currents due to the reduction of oxygen were observed using rotating ring disk electrodes, as shown in Figure 5A. A shift of 50 mV to a more positive potential of the current at Pt/PW-SWCNT indicated its higher catalytic activity compared to that of Pt/CB. Further analysis related to the temperature dependence of the reaction allows us to determine the rate constant (k_{app}) for oxygen reduction. Pt/PW-SWCNT revealed an activity enhancement factor of 2 in comparison to Pt/CB (see Supporting Information Figure S2). This is a comparable to that on the Pt-based alloy particle deposited on carbon black.[35−37] Peroxide yields during the oxygen reduction were recorded at the ring electrode, as shown in Figure 5B. The yields are small (1−3%) and comparable for both Pt/PW-SWCNT and Pt/CB, indicating that the reaction pathways are identical. The significant performance of Pt/PW-SWCNT as an electrocatalyst is a strong indication that the influence of PSS on the electron conductivity of SWCNT is negligible.

It is known that the d-band level of Pt plays an important role and that an appropriate d-band vacancy is required to optimize the catalytic activity in oxygen reduction. The d-band vacancy of Pt could be varied by depositing Pt on a metal substrate[38,39] or by alloying.[35,36,40,41] Considering the work functions are 4.73 eV for individual SWCNTs and ∼5 eV for bundled SWCNTs,[42,43] it is reasonable that SWCNTs can enhance the d vacancy of Pt (Φ_{Pt} = 5.36 eV) and improve the activity of oxygen reduction. X-ray photoelectron spectroscopy was employed to investigate the binding energy of d-band electrons of Pt. As shown in Figure 6, a shift of ∼0.4 eV to a higher binding energy was found in both 4d and 4f electrons of

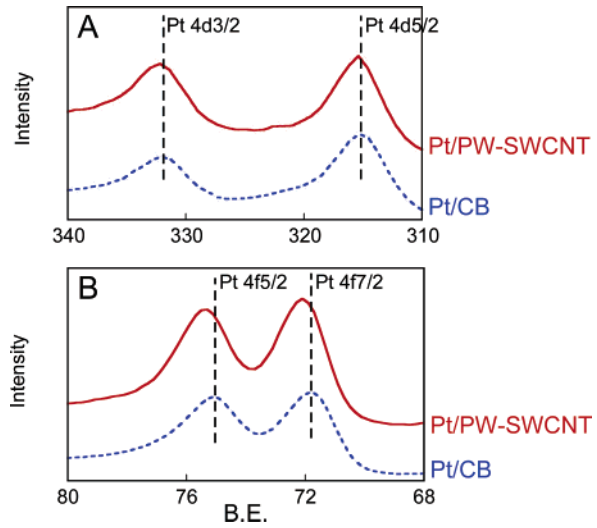

Figure 6. X-ray photoelectron spectroscopy of Pt of Pt/PW-SWCNT compared with Pt/CB.

Pt deposited on PW-SWCNT, proving the role of SWCNTs in modifying the electronic properties of Pt.

Conclusions

In summary, we have reported here a successful method to deposit Pt nanoparticles on small bundles of SWCNTs with good dispersion, using the polymer-wrapping technique. With this method, it was shown that SWCNTs retain their basis properties and can promote electrocatalytic reaction in both kinetics and mass transfer. Catalytic activity for oxygen reduction increases by a factor of 2 when using Pt/PW-SWCNT. This is comparable to those of Pt-based alloys; however, Pt/PW-SWCNT yet has the advantage of its single-component system that it has a lower H_2O_2 production rate and has a higher stability than those of the alloys. A 3-fold higher diffusion rate of methanol was observed during methanol oxidation, which can be related to the ballistic diffusion occurring inside the nanotubes. X-ray photoelectron spectroscopy (XPS) revealed the SWCNT shift of the d-band center of Pt to a lower level which enhances the activity of oxygen reduction. This study demonstrates a way to utilize SWCNTs in fabricating high performance electrocatalysts.

Acknowledgment. We would like to thank Dr. Takao Sakata for his assistance in recording the TEM images and Prof. Yasuhiro Tachibana for helpful discussions. The research described herein was supported by the Indiana 21st Century Research and Technology Fund and the U.S. Army CECOM RDEC through Agreement DAAB07-03-3-K414. Such support does not constitute endorsement by the U.S. Army of the views expressed in this publication. This is Contribution No. NDRL 4673 from Notre Dame Radiation Laboratory.

Supporting Information Available: Additional TEM images of Pt/PW-SWCNT (Figure S1) and Arrhenius plots to determine the apparent rate constant for oxygen reduction on Pt/PW-SWCNT (Figure S2). This material is available free of charge via the Internet at http://pubs.acs.org.

References and Notes

(1) Tans, S. J.; Devoret, M. H.; Dai, H. J.; Thess, A.; Smalley, R. E.; Geerligs, L. J.; Dekker, C. *Nature* **1997**, *386*, 474.
(2) Morales, A. M.; Lieber, C. M. *Science* **1998**, *279*, 208.
(3) Tans, S. J.; Verschueren, A. R. M.; Dekker, C. *Nature* **1998**, *393*, 49.
(4) Martel, R.; Schmidt, T.; Shea, H. R.; Hertel, T.; Avouris, P. *Appl. Phys. Lett.* **1998**, *73*, 2447.
(5) Hummer, G.; Rasaiah, J. C.; Noworyta, J. P. *Nature* **2001**, *414*, 188.
(6) Brovchenko, I.; Geiger, A.; Oleinikova, A. *Phys. Chem. Chem. Phys.* **2001**, *3*, 1567.
(7) Mao, Z. G.; Sinnott, S. B. *J. Phys. Chem. B* **2000**, *104*, 4618.
(8) Skoulidas, A. I.; Ackerman, D. M.; Johnson, J. K.; Sholl, D. S. *Phys. Rev. Lett.* **2002**, *89*, 185901.
(9) Mao, Z. G.; Sinnott, S. B. *J. Phys. Chemistry B* **2001**, *105*, 6916.
(10) Girishkumar, G.; Vinodgopal, K.; Kamat, P. V. *J. Phys. Chem. B* **2004**, *108*, 19960.
(11) Girishkumar, G.; Rettker, M.; Underhile, R.; Binz, D.; Vinodgopal, K.; McGinn, P.; Kamat, P. *Langmuir* **2005**, *21*, 8487.
(12) Girishkumar, G.; Hall, T. D.; Vinodgopal, K.; Kamat, P. V. *J. Phys. Chem. B* **2006**, *110*, 107.
(13) Che, G.; Lakshmi, B. B.; Martin, C. R.; Fisher, E. R. *Langmuir* **1999**, *15*, 750.
(14) Steigerwalt, E. S.; Deluga, G. A.; Lukehart, C. M. *J. Phys. Chem. B* **2002**, *106*, 760.
(15) Kim, C.; Kim, Y. J.; Kim, Y. A.; Yanagisawa, T.; Park, K. C.; Endo, M. *J. Appl. Phys.* **2004**, *96*, 5903.
(16) Sun, X.; Li, R.; Villers, D.; Dodelet, J. P.; Desilets, S. *Chem. Phys. Lett.* **2003**, *379*, 99.
(17) Wang, X.; Waje, M.; Yan, Y. *Electrochem. Solid State Lett.* **2005**, *8*, A42.
(18) Mu, Y. Y.; Liang, H. P.; Hu, J. S.; Jiang, L.; Wan, L. J. *J. Phys. Chem. B* **2005**, *109*, 22212.
(19) Kongkanand, A.; Kuwabata, S.; Girishkumar, G.; Kamat, P. *Langmuir* **2006**, *22*, 2392.
(20) Yu, R. Q.; Chen, L. W.; Liu, Q. P.; Lin, J. Y.; Tan, K. L.; Ng, S. C.; Chan, H. S. O.; Xu, G. Q.; Hor, T. S. A. *Chem. Mater.* **1998**, *10*, 718.
(21) O'Connell, M. J.; Bachilo, S. M.; Huffman, C. B.; Moore, V. C.; Strano, M. S.; Haroz, E. H.; Rialon, K. L.; Boul, P. J.; Noon, W. H.; Kittrell, C.; Ma, J. P.; Hauge, R. H.; Weisman, R. B.; Smalley, R. E. *Science* **2002**, *297*, 593.
(22) Moore, V. C.; Strano, M. S.; Haroz, E. H.; Hauge, R. H.; Smalley, R. E.; Schmidt, J.; Talmon, Y. *Nano Lett.* **2003**, *3*, 1379.
(23) O'Connell, M. J.; Boul, P.; Ericson, L. M.; Huffman, C.; Wang, Y. H.; Haroz, E.; Kuper, C.; Tour, J.; Ausman, K. D.; Smalley, R. E. *Chem. Phys. Lett.* **2001**, *342*, 265.
(24) Liu, J.; Casavant, M. J.; Cox, M.; Walters, D. A.; Boul, P.; Lu, W.; Rimberg, A. J.; Smith, K. A.; Colbert, D. T.; Smalley, R. E. *Chem. Phys. Lett.* **1999**, *303*, 125.
(25) Wang, Y.; Ren, J. W.; Deng, K.; Gui, L. L.; Tang, Y. Q. *Chem. Mater.* **2000**, *12*, 1622.
(26) Bock, C.; Paquet, C.; Couillard, M.; Botton, G. A.; MacDougall, B. R. *J. Am. Chem. Soc.* **2004**, *126*, 8028.
(27) Li, X.; Ge, S.; Hui, C. L.; Hsing, I.-M. *Electrochem. Solid State Lett.* **2004**, *7*, A286.
(28) Li, W.; Liang, C.; Zhou, W.; Qiu, J.; Zhou, Z.; Sun, G.; Xin, Q. *J. Phys. Chem. B* **2003**, *107*, 6292.
(29) Xing, Y. *J. Phys. Chem. B* **2004**, *108*, 19255.
(30) Tian, Z. Q.; Jiang, S. P.; Liang, Y. M.; Shen, P. K. *J. Phys. Chem. B* **2006**, *110*, 5343.
(31) Dresselhaus, M. S.; Dresselhaus, G.; Jorio, A.; Filho, A. G. S.; Pimenta, M. A.; Saito, R. *Acc. Chem. Res.* **2002**, *35*, 1070.
(32) Jorio, A.; Pimenta, M. A.; Filho, A. G. S.; Saito, R.; Dresselhaus, G.; Dresselhaus, M. S. *New J. Phys.* **2003**, *5*, 139.
(33) Heller, D. A.; Barone, P. W.; Swanson, J. P.; Mayrhofer, R. M.; Strano, M. S. *J. Phys. Chem. B* **2004**, *108*, 6905.
(34) Li, W.; Wang, X.; Chen, Z.; Waje, M.; Yan, Y. Pt-Ru Supported on Double-Walled Carbon Nanotubes as High-Performance Anode Catalysts for Direct Methanol Fuel Cells. *J. Phys. Chem. B*, in press.
(35) Paulus, U. A.; Wokaun, A.; Scherer, G. G.; Schmidt, T. J.; Stamenkovic, V.; Markovic, N. M.; Ross, P. N. *Electrochim. Acta* **2002**, *47*, 3787.
(36) Stamenkovic, V.; Schmidt, T. J.; Ross, P. N.; Markovic, N. M. *J. Phys. Chem. B* **2002**, *106*, 11970.
(37) Paulus, U. A.; Wokaun, A.; Scherer, G. G.; Schmidt, T. J.; Stamenkovic, V.; Radmilovic, V.; Markovic, N. M.; Ross, P. N. *J. Phys. Chem. B* **2002**, *106*, 4181.
(38) Ruban, A.; Hammer, B.; Stoltze, P.; Skriver, H. L.; Norskov, J. K. *J. Mol. Catal. A* **1997**, *115*, 421.
(39) Pedersen, M. O.; Helveg, S.; Ruban, A.; Stensgaard, I.; Lagsgaard, E.; Norskov, J. K.; Besenbacher, F. *Surf. Sci.* **1999**, *426*, 395.
(40) Toda, T.; Igarashi, H.; Uchida, H.; Watanabe, M. *J. Electrochem. Soc.* **1999**, *146*, 3750.
(41) Igarashi, H.; Fujino, T.; Zhu, Y.; Uchida, H.; Watanabe, M. *Phys. Chem. Chem. Phys.* **2001**, *3*, 306.
(42) Zhao, J. J.; Han, J.; Lu, J. P. *Phys. Rev. B* **2002**, *65*, 193401.
(43) Suzuki, S.; Watanabe, Y.; Homma, Y.; Fukuba, S.; Heun, S.; Locatelli, A. *Appl. Phys. Lett.* **2004**, *85*, 127.